Spin Ladders

DOI: 10.1002/ange.200801146

Spin-Ladder Iron Oxide: $Sr_3Fe_2O_5$**

Hiroshi Kageyama, Takashi Watanabe, Yoshihiro Tsujimoto, Atsushi Kitada, Yuji Sumida, Kazuyoshi Kanamori, Kazuyoshi Yoshimura, Naoaki Hayashi, Shigetoshi Muranaka, Mikio Takano, Monica Ceretti, Werner Paulus, Clemens Ritter, and Gilles André*

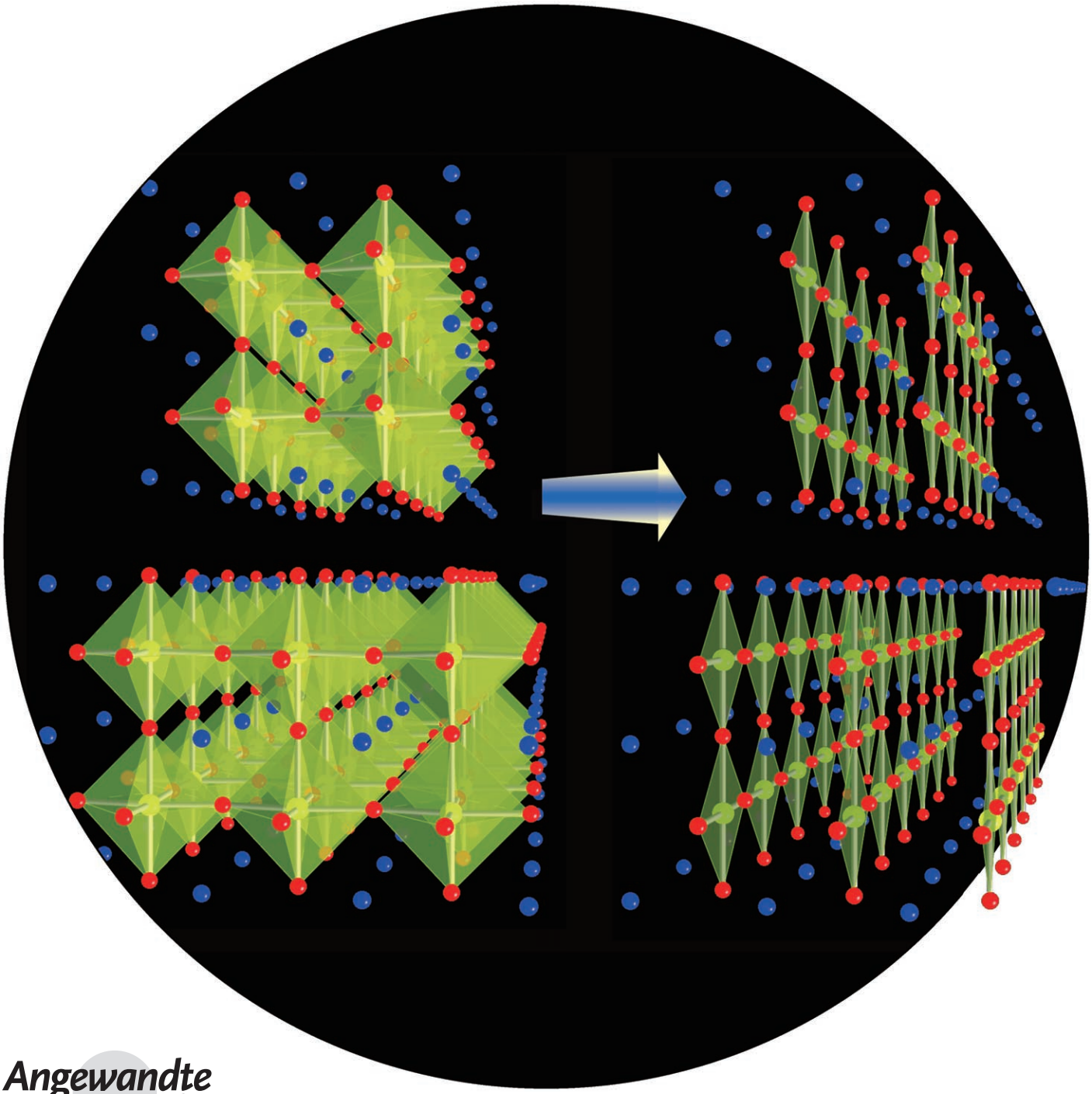

Spin ladders, which conceptually are unidirectional sections of an antiferromagnetic (AF) two-dimensional (2D) square lattice, as schematically illustrated in Figure 1, have attracted considerable attention in the last two decades. Theories predict that the ground state of an $S=1/2$ ladder is a gapped singlet spin liquid state when the leg number n is even, but is a gapless singlet spin liquid state when n is odd.[1] Moreover, short-range AF spin correlation should lead to superconductivity when modest carriers are doped in even-legged ladders. Experimental counterparts are the observation of the gapped and gapless ground states of $SrCu_2O_3$ ($n=2$) and $Sr_2Cu_3O_5$ ($n=3$), respectively,[2] and the appearance of superconductivity in $(Sr,Ca)_{14}Cu_{24}O_{41+x}$ ($n=2$) under high pressure.[3] Another $S=1/2$ two-legged Cu^{2+} ladder, namely, $La_{1-x}Sr_xCuO_{2.5}$, shows anomalous behavior associated with its nearly critical ground state.[4]

The motivation of theoretical investigations has been to test how the one-dimensional (1D) $S=1/2$ AF chain system ($n=1$), which is rigorously solved even when doped with carriers, can be related to the 2D square lattice ($n=\infty$), which presents various theoretical difficulties and is far from being understood. Experimentally, $Sr_{n-1}Cu_nO_{2n-1}$ is the only example of a generalized spin-ladder system,[5] though the composition and structure of a two-legged ladder has been extended to CaV_2O_5, $Cu_2(C_5H_{12}N_2)Cl_4$, $(C_5H_{12}N)_2CuBr_4$, $[Ph(NH_3)$-$([18]crown-6)][Ni(dmit)_2]$ (dmit = dithiolene) and $[(DT$-$TTF)_2][Au(mnt)_2]$ (DT-TTF = dithiophene tetrathiafulvalene, mnt = maleonitrile dithiolate).[6] It is highly desirable from both theoretical and experimental viewpoints to extend these ladder systems with respect to n and S, and also with respect to possible skews such as mixing of ferromagnetic and AF interactions. An example of skew is the dramatic switching of the large-gapped (> 400 K) singlet spin liquid of $SrCu_2O_3$ to an AF ordered state by the nonmagnetic substituent Zn^{2+}, even at $Zn/Cu \leq 1\,\%$.[7]

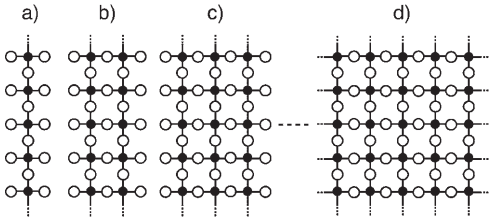

Figure 1. Spin ladders with n legs; solid and open circles denote magnetic ions and oxide ions, respectively. a) One-legged spin ladder (i.e., the 1D chain). b) Two-legged spin ladder realized in the present work. c) Three-legged spin ladder. d) ∞-legged spin ladder (i.e., the 2D square lattice) realized in $SrFeO_2$.[9]

The most pronounced structural characteristic of d^9 copper(II) oxides is the favored formation of square-planar CuO_4 units, which are stabilized due to the Jahn–Teller effect.[8] This 2D coordination geometry provides strong Cu-O-Cu superexchange interactions within a ladder along the legs and rungs, while Cu···Cu interactions normal to the square plane ($\| z$) are negligibly small because the copper(II) ions have a magnetically inert, filled ($d_{z^2}\uparrow\downarrow$) configuration along this direction and also because an intervening oxygen atom is lacking.

Unlike the case of cuprates, the coordination geometries in iron oxides have been almost exclusively restricted to 3D polyhedra such as octahedra and tetrahedra. However, this restriction was recently overcome[9] by using calcium hydride at low temperatures as a reductant, as initiated and developed by Hayward, Rosseinsky and co-workers.[10,11] Low-temperature reaction of cubic perovskite $SrFe^{IV}O_3$ with CaH_2 led to stable $SrFe^{II}O_2$ with a square-planar oxygen coordination environment around the high-spin Fe^{2+} ion. The structure is isostructural with the "infinite"-layer cupric oxides.[12] Herein we report the synthesis of novel spin-ladder iron oxide $Sr_3Fe^{II}{}_2O_5$ through reaction of double-layered perovskite $Sr_3Fe^{IV}{}_2O_7$ with CaH_2. Together with the synthesis of $SrFeO_2$, this opens up new avenues for the solid-state chemistry of iron(II) oxides with square-planar coordination, which potentially includes the serial ladder system $Sr_{n+1}Fe_nO_{2n+1}$, and for the solid-state physics of multiple-spin ladders.

The slightly oxygen-deficient phase $Sr_3Fe_2O_{7-y}$ ($y\approx 0.4$), which can be prepared easily by a conventional, high-temperature solid-state reaction, was used as precursor. It is known that all oxygen vacancies are located at the apical O(1) sites shared by the double FeO_2 sheets (Figure 2a and b) and that the structure keeps the $I4/mmm$ space group over the entire range from $Sr_3Fe_2O_7$ ($y=0$) to $Sr_3Fe_2O_6$ ($y=1$).[13] The lattice parameters of the as-obtained precursor determined by powder X-ray diffraction (XRD) were $a=3.872$ and $c=$

[*] Prof. Dr. H. Kageyama, T. Watanabe, Y. Tsujimoto, A. Kitada, Y. Sumida, Dr. K. Kanamori, Prof. Dr. K. Yoshimura
Department of Chemistry, Graduate School of Science
Kyoto University, Kyoto 606-8502 (Japan)
Fax: (+81) 75-753-3991
E-mail: kage@kuchem.kyoto-u.ac.jp
Homepage: http://kuchem.kyoto-u.ac.jp/kinso/kage/index_-eng.html
Dr. N. Hayashi, Prof. Dr. S. Muranaka
Graduate School of Human and Environmental Studies
Kyoto University (Japan)
Prof. Dr. M. Takano
Institute for Chemical Research, Kyoto University (Japan)
and
Institute for Integrated Cell-Materials Sciences and
Research Institute for Production Development, Kyoto (Japan)
Dr. M. Ceretti, Prof. Dr. W. Paulus
Université de Rennes 1, UMR CNRS 6226 (France)
Dr. C. Ritter
Institute Laue Langevin, Grenoble (France)
Dr. G. André
Laboratoire Léon Brillouin, CEA-CNRS, Gif-sur-Yvette (France)

[**] We thank Dr. K. Kato for his precious help with the measurements at SPring-8, E. Fukui and K. Nakanishi for their help with the TG measurements, and M. Nishi and N. Nagaosa for helpful discussions. The synchrotron radiation experiments were performed at Spring-8 with the approval of the Japan Synchrotron Radiation Research Institute. This work was supported by Young Scientists A (H.K), the Grant-in-Aid for Scientific Research on Priority Areas (H.K. and K.Y.) and Scientific Research S (M.T.) from MEXT, and by GCOE program, Kyoto University.

Supporting information for this article is available on the WWW under http://dx.doi.org/10.1002/anie.200801146.

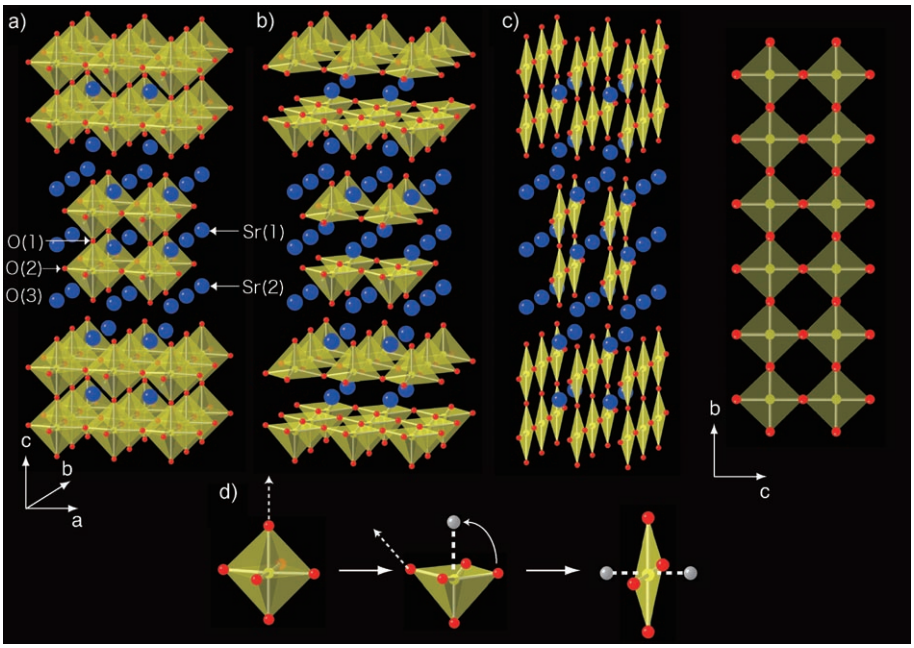

Figure 2. Structural transformation from $Sr_3Fe_2O_7$ to $Sr_3Fe_2O_5$ via $Sr_3Fe_2O_6$, where the blue, red, and yellow spheres represent Sr, O, and Fe atoms, respectively. a) Crystal structure of a stoichiometric (fully oxidized) phase $Sr_3Fe_2O_7$ ($y=0$). b) Crystal structure of reduced phase $Sr_3Fe_2O_6$ ($y=1$), once thought to be the lower limit of the oxygen content. c) Left: Crystal structure of the new phase $Sr_3Fe_2O_5$ ($y=2$), described herein. Right: A spin ladder in $Sr_3Fe_2O_5$ viewed along the *a* axis. d) Transformation from the octahedron (left) in $Sr_3Fe_2O_7$ to the pyramid (middle) in $Sr_3Fe_2O_6$ and to the square plane (right) in $Sr_3Fe_2O_5$, where the white spheres represent oxygen vacancies.

20.157 Å, corresponding to a phase with $Sr_3Fe_2O_{6.6}$ stoichiometry. Note that $Sr_3Fe^{III}{}_2O_6$ ($y=1$) is thought to represent the lower end of the oxygen stoichiometry, in spite of intensive studies owing to their interesting properties such as metal–insulator transition, charge disproportionation, and possible applications as oxygen-separation membranes and solid-oxide fuel cells.[14]

Reduction of $Sr_3Fe_2O_{6.6}$ with CaH_2 was performed in an evacuated glass tube at 623 K for 3 d. As shown in Figure 3, the room-temperature synchrotron powder XRD pattern of the final product was readily indexed with an *I*-centered orthorhombic unit cell with $a=3.51485(2)$, $b=3.95271(2)$, and $c=20.91251(10)$ Å, except for a very minor unknown impurity (see Figure S1 in the Supporting Information). Compared to $Sr_3Fe_2O_{6.6}$, the *b* axis remained nearly unchanged, while the *a* axis (*c* axis) substantially decreased (increased). The *a* axis is of similar length to the *c* axis of $SrFeO_2$ ($a=b=3.99$ Å, $c=3.47$ Å).[6] These observations strongly suggested that the FeO_2 in-plane oxygen atoms O(2) along the *a* axis were all removed, while the apical oxygen sites O(1) were filled up, resulting in the formation of $Sr_3Fe_2O_5$ crystallizing in space group *Immm* (Figure 2c). The Rietveld refinement based on this model immediately converged to $R_{wp}=0.0524$ and $\chi^2=5.28$ along with reasonable individual isotropic displacement factors for all atoms. The bond valence sum calculation gave +1.88, +1.86, and +1.95 for Sr(1), Sr(2), and Fe, consistent with the expected valences of +2 for these elements. Neutron powder diffraction (NPD) analysis at 293 K confirmed the above structure model, with an excellent convergence of $R_{wp}=0.0376$ and $\chi^2=2.78$ (see Figure S2 in the Supporting Information). We tried to refine the oxygen occupancies and found that all O(1), O(2), and O(3) sites are fully occupied within 1% error, and no extra oxygen atoms could be found. It also excluded possible hydrogen incorporation into the lattice, as found in $LaSrCoO_3H_{0.7}$.[11] The three types of Fe–O bonds ($d_{Fe-O(1)}=2.013$ (one bond), $d_{Fe-O(2)}=1.976$ (two bonds), $d_{Fe-O(3)}=2.039$ Å (one bond)) form a nearly square FeO_4 plane.

Furthermore, Mössbauer measurements (Figure 4a) indicated not only that all the Fe atoms are electronically and crystallographically equivalent, but also that they are most likely square-planar coordinated in high-spin state ($S=2$), since the obtained isomer shift (IS) of 0.46 mm s^{-1}, quadrupole splitting ΔE of 1.28 mm s^{-1} at 297 K, and the magnetic hyperfine field of $H_{hf}=43.7$ T at 4 K are close to those of $SrFeO_2$.[9] These observations are consistent with the structural analysis. Thermogravimetric

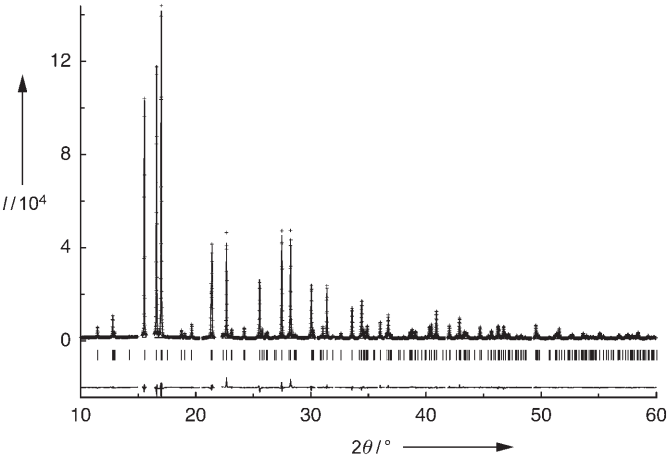

Figure 3. Structural characterization of $Sr_3Fe_2O_5$ by Rietveld refinement of synchrotron XRD data at 293 K. The overlying crosses, solid lines, and ticks represent the observed and calculated intensities and the position of the calculated Bragg reflections, respectively. The difference between the calculated and observed profiles is plotted at the bottom. $Sr_3Fe_2O_5$ adopts the *Immm* space group (No. 71), $a=3.514825(2)$, $b=3.95271(2)$, $c=20.91252(10)$ Å, $Z=2$. Sr(1) on 2*c* (0.5,0.5,0), Sr(2) on 4*i* (0,0,0.31234(2)), Fe on 4*i* (0,0,0.09636(2)), O(1) on 2*a* (0,0,0), O(2) on 4*j* (0.5,0,0.59574), O(3) on 4*i* (0,0,0.19358(2)), with 100% occupancy, $B_{iso}(Sr(1))=0.359(22)$ Å^2, $B_{iso}(Sr(2))=0.213(13)$ Å^2, $B_{iso}(Fe)=0.089(16)$ Å^2, $B_{iso}(O(1))=0.12(11)$ Å^2, $B_{iso}(O(2))=0.15(6)$ Å^2, $B_{iso}(O(3))=0.59(8)$ Å^2, $R_p=0.0401$, $R_{wp}=0.0524$,and $\chi^2=5.28$. Refining the occupation factors at the oxygen sites and the vacant site did not improve the result.

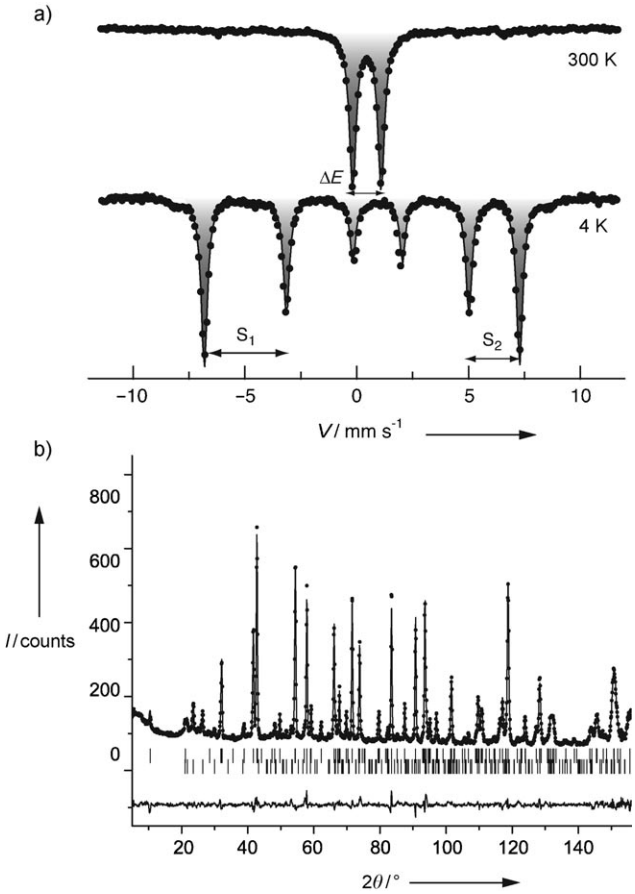

Figure 4. Magnetic order in $Sr_3Fe_2O_5$. a) Mössbauer spectra at 300 (top) and 4 K (bottom). The circles indicate the experimental data, while the lines denote the fits. b) Rietveld refinement of NPD data at 10 K measured at 1.91 Å. The solid lines and the overlying crosses and bars indicate the calculated intensities, the observed intensities, and the positions of the calculated chemical (top) and magnetic (bottom) Bragg reflections. The difference between the observed and calculated profiles is plotted at the bottom. See Tables S1 and S2 in the Supporting Information for details.

(TG) measurements showed the oxygen content of the product to be less than 6 (i.e., $y>1$) though its precise determination was hampered by partial reactions (oxidation, decomposition, hydration) of $Sr_3Fe_2O_5$ while it was exposed to air for the experimental setup (see Figure S3 in the Supporting Information).

When half of the O(2) sites in $Sr_3Fe_2O_7$ are removed in the present ordered manner, the original double perovskite layers become decoupled into ladders with two legs running along [010] and rungs along [001] (Figure 2c). $Sr_3Fe_2O_5$ and $SrFeO_2$ are thus two- and ∞-legged $S=2$ ladder compounds, respectively. The sectioning of the dense FeO_2 sheet in $SrFeO_2$ into the two-legged ladders loosely distributed in $Sr_3Fe_2O_5$ should greatly change the magnetism, at least by drastically lowering the 3D magnetic ordering temperature. Indeed, the NPD pattern of $Sr_3Fe_2O_5$ at 293 K does not contain any magnetic reflections, and the Mössbauer spectrum at 300 K just consists of a quadruple doublet, that is, $Sr_3Fe_2O_5$ is still in the paramagnetic state, in contrast to the case of $SrFeO_2$ with T_N as high as 473 K. In the Mössbauer spectrum at 4 K (Figure 4a), however, we found a sharp sextet, clearly indicative of long-range AF order. Furthermore, the NPD data at 10 K (Figure 4b) revealed that the long-range AF order is characterized by a magnetic propagation vector $q=$ (1/2, 1/2, 0) and that the iron moments of 2.76(5) μ_B are aligned parallel to the c axis (see Figure 4S in the Supporting Information). This so-called G-type antiferromagnetic structure is frequently observed in double-layered Ruddlesden–Popper phases such as $Sr_3Mn_2O_7$.[15] The fact that the Fe moment is reduced by more than 20% from that of 3.6 μ_B for $SrFeO_2$ must be a consequence of a quantum magnetic fluctuation enhanced inherently in the ladder, though future theoretical support is needed.

Considering that $Sr_3Fe_2O_7$ and $SrFeO_3$ are the $n=2$ and $n=\infty$ members of a homologous series $Sr_{n+1}Fe_nO_{3n+1}$, where n represents the number of perovskite blocks,[13] we can predict a new homologous n-legged $S=2$ ladder series $Sr_{n+1}Fe_nO_{2n+1}$ (Figure 1). In this context, the reaction of Sr_2FeO_4 ($n=1$) and $Sr_4Fe_3O_{10}$ ($n=3$) with CaH_2 should result in the one-legged ladder (i.e., 1D chain) compound Sr_2FeO_3 and the three-legged ladder compound $Sr_4Fe_3O_7$, respectively (see Figure S5 in the Supporting Information). This work is in progress. Note that $(LaSr_3)(Fe_{1.5}Co_{1.5})O_{7.5}$, obtained by hydride reduction of the $n=3$ La- and Co-substituted sample $(LaSr_3)(Fe_{1.5}Co_{1.5})O_{10}$, has a different framework composed of three-coordinate metal ions flanked by square-based pyramidal coordination,[10d] instead of the three-legged ladder solely with square-planar coordination.

It is also interesting to compare the copper(II) and iron(II) ladder systems $Sr_{n-1}Cu_nO_{2n-1}$[5] and $Sr_{n+1}Fe_nO_{2n+1}$. In the former, the ladders, each having the composition Cu_nO_{2n-1}, share their O–O edges to form the dense Cu_nO_{2n-1} sheet. The iron(II) ladders, on the other hand, are dispersed in the I-centered orthorhombic lattice with their legs and rungs oriented along the b and c axes, respectively. The linear Fe-O-Fe bonds are strong and AF, as found for $SrFeO_2$. As a consequence, the phase shift along the leg direction by $\pi/2$ between the corner and center ladders should minimize their interactions by spin frustration, as in the dense Cu_nO_{2n-1} sheet. However, if the electronic configuration of the FeO_4 unit is $(d_{yz},d_{zx})^3(d_{xy})^1(d_{z^2})^1(d_{x^2-y^2})^1$ with $S=2$, as proposed for $SrFeO_2$, the iron(II) ladders facing each other in phase along the a axis should interact more strongly in an AF $Fe(d_{z^2}\uparrow)\cdots Fe(d_{z^2}\downarrow)$ manner than the corresponding Cu$\cdots$Cu interactions, because these copper(II) ions have an inert, filled ($d_{z^2}\uparrow\downarrow$) configuration. Numerical calculations for a $S=1/2$ two-legged ladder system showed that the gapped spin liquid state can be replaced by an ordered state at a critical value of $J'/J\approx 0.11$, where J and J' are the intra- and interladder exchange interactions, respectively.[4b] There are no calculations for $S=2$ systems, but there is no doubt that the magnetic order in $Sr_3Fe_2O_5$ results mainly from interactions along the a axis.

The mechanism of reduction from $Sr_3Fe_2O_7$ to $Sr_3Fe_2O_5$ merits detailed inspection. We tried to slow down the process by lowering the synthesis temperature to 553 K. Interruption of the reaction after one day resulted in $Sr_3Fe_2O_6$, while a one-week reaction at the same temperature yielded $Sr_3Fe_2O_5$, that is, the process is two-staged. The first step from $Sr_3Fe_2O_7$ to

$Sr_3Fe_2O_6$ is nothing but continuous randomized removal of the O(1) ions leading to a coordination change from FeO_6 octahedra to FeO_5 square pyramids. This is quite common for the $n=2$ Ruddlesden–Popper phases and there is nothing special in the present case. However, the second step, the transformation of the FeO_5 square pyramids in $Sr_3Fe_2O_6$ into the FeO_4 squares in $Sr_3Fe_2O_5$ must be more complicated and cooperative. Supposing one basal oxygen atom of a given square pyramid escapes into the reducing atmosphere, another basal oxygen atom must move up to the vacant apical site, as illustrated in Figure 2d, and these processes should take place cooperatively over a certain lattice volume for crystallization. Thus, the reduction mechanism changes at $y=1$.

It is noteworthy that there are neither intermediate phases nor nonstoichiometry between $Sr_3Fe_2O_6$ and $Sr_3Fe_2O_5$, as well as between $SrFeO_{2.5}$ and $SrFeO_2$. This is remarkable given the presence of two intermediates, $SrFeO_{2.875}$ and $SrFeO_{2.75}$, between $SrFeO_3$ and $SrFeO_{2.5}$. It is also known that electrochemical formation of $SrCoO_3$ from $SrCoO_{2.5}$, which are isomorphous with $SrFeO_3$ and $SrFeO_{2.5}$, respectively, proceeds topotactically at room-temperature via the complex vacancy-ordered intermediate phase $SrCoO_{2.82\pm0.07}$.[16] The processes occurring in the formation of $SrFeO_2$ from $SrFeO_{2.5}$, whereby the FeO_4 tetrahedra and the FeO_6 octahedra linked to each other are both converted to FeO_4 squares[17] must be more complicated than the case discussed above. We now recognize that the underlying perovskite and related lattices are flexible enough to tolerate such drastic compositional and structural events. We thus believe that oxygen-transport materials working at low temperatures that feature formation of intermediate ordered structures should be promising.

Finally, we must assume that the present synthetic strategy involving CaH_2 reduction can be further generalized for a more rational design of new magnetic lattices comprising extended arrays of FeO_4 square planes, for which formerly only copper(II) oxides were candidates. It would also be interesting to test other transition metal oxides.

Experimental Section

Precursor $Sr_3Fe_2O_{7-y}$ ($y\approx0.4$) was prepared by a conventional high-temperature ceramic method from predried $SrCO_3$ (99.99%) and Fe_2O_3 (99.99%) by heating a pelletized stoichiometric mixture of these at 1273 K in air for 24 h and again for 24 h at 1473 K after grinding and pelletization. The reduction of $Sr_3Fe_2O_{7-y}$ ($y\approx0.4$) was performed with CaH_2 as reducing agent. $Sr_3Fe_2O_{7-y}$ (0.43 g) and a four-molar excess of CaH_2 (0.15 g) were finely ground in an Ar-filled glove box, sealed in an evacuated pyrex tube ($V=15\ cm^3$) with a residual pressure of less than 1.3×10^{-2} Pa, and heated at 623 K for 3 d. Residual CaH_2 and the CaO byproduct were removed from the final reaction phase by washing with 0.1M NH_4Cl in dried methanol. $Sr_3Fe_2O_5$ is air-sensitive, in contrast to $SrFeO_2$.

Thermogravimetric measurements were performed with a thermal analyzer (Rigaku Thermoplus TG8120). Measurements to analyze reoxidation behavior of $Sr_3Fe_2O_5$ were performed on a sample of around 10 mg that was rapidly loaded into a platinum crucible and then heated at 10 K min^{-1} in air. Prior to the experiment, the sample was dried at 373 K for about 1 h. The identity of the reoxidized product was determined by powder X-ray diffraction.

The synchrotron powder XRD experiment was performed on the large Debye–Scherrer camera installed at SPring-8 BL02B2 by using an imaging plate as detector. Incident beams from a bending magnet were monochromatized to 0.77709 Å. The sample was contained in a glass capillary tube with an inner diameter of 0.1 mm and was rotated during measurements. The diffraction data were collected at room temperature in a 2θ range from 1 to 75° with a step interval of 0.01°. The NPD studies were carried out on the D1A diffractometer installed at the Institute Laue Langevin (Grenoble, France). A 250-mg sample sealed in an He-filled vanadium can was used, and a wavelength of $\lambda=1.91$ Å was employed.

Mössbauer spectra were taken in transmission geometry by using a ^{57}Co/Rh γ-ray source kept at room temperature on a powdered sample of $Sr_3Fe_2O_5$. The source velocity was calibrated by using pure α-Fe as control material, and the isomer shift is relative to α-Fe. The spectra were fitted by using the Lorentzian function.

The XRD and NPD patterns were analyzed by the Rietveld method with RIETAN 2000[18] and FULLPROF software,[19] respectively. The agreement indices used were the weighted profile $R_{wp}=[\Sigma w_i(y_{io}-y_{ic})^2/\Sigma w_i(y_{io})^2]^{1/2}$ and the goodness of fit (GOF), $\chi^2=(R_{wp}/R_{exp})^2$, where $R_{exp}=[(N-P)/\Sigma w_i y_{io}{}^2]^{1/2}$, y_{io} and y_{ic} are the observed and calculated intensities, w_i is the weighting factor, N the total number of y_{io} data when the background is refined, and P the number of adjusted parameters. The bond valence sum method was applied to estimate the valence of cations by using tabulated parameters.[20]

Received: March 10, 2008
Revised: May 14, 2008

Keywords: iron · layered compounds · perovskite phases · reduction · spin ladders

[1] a) E. Dagotto, T. M. Rice, *Science* **1996**, *271*, 618–623; b) E. Dagotto, *Rep. Prog. Phys.* **1999**, *62*, 1525–1571.
[2] a) M. Azuma, Z. Hiroi, M. Takano, K. Ishida, Y. Kitaoka, *Phys. Rev. Lett.* **1994**, *73*, 3463–3466; b) K. Kojima, A. Keren, G. M. Luke, B. Nachumi, W. D. Wu, Y. J. Uemura, M. Azuma, M. Takano, *Phys. Rev. Lett.* **1995**, *74*, 2812–2815.
[3] a) M. Uehara, T. Nagata, J. Akimitsu, H. Takahashi, N. Mori, K. Kinoshita, *J. Phys. Soc. Jpn.* **1996**, *65*, 2764–2767; b) T. Vuletić, B. Korin-Hamzić, T. Ivek, S. Tomić, B. Gorshunov, M. Dressel, J. Akimitsu, *Phys. Rep.* **2006**, *428*, 169–258.
[4] a) Z. Hiroi, M. Takano, *Nature* **1995**, *377*, 41–43; b) M. Troyer, M. E. Zhitomirsky, K. Ueda, *Phys. Rev. B* **1997**, *55*, R6117–R6120.
[5] Z. Hiroi, M. Azuma, M. Takano, Y. Bando, *J. Solid State Chem.* **1991**, *95*, 230–238.
[6] a) Y. Ueda, *Chem. Mater.* **1998**, *10*, 2653–2664; b) B. Chiari, O. Piovesana, T. Tarantelli, P. F. Zanazzi, *Inorg. Chem.* **1990**, *29*, 1172–1176; c) C. Rovira, *Chem. Eur. J.* **2000**, *6*, 1723–1729; d) Y. Hosokoshi, K. Katoh, Y. Nakazawa, H. Nakano, K. Inoue, *J. Am. Chem. Soc.* **2001**, *123*, 7921–7922.
[7] M. Azuma, Y. Fujishiro, M. Takano, M. Nohara, H. Takagi, *Phys. Rev. B* **1997**, *55*, R8658–R8861.
[8] A. F. Wells, *Structural Inorganic Chemistry*, 3rd ed., Oxford University Press, Oxford, UK, **1962**.
[9] Y. Tsujimoto, C. Tassel, N. Hayashi, T. Watanabe, H. Kageyama, K. Yoshimura, M. Takano, M. Ceretti, C. Ritter, W. Paulus, *Nature* **2007**, *450*, 1062–1065.
[10] a) M. A. Hayward, M. A. Green, M. J. Rosseinsky, J. Sloan, *J. Am. Chem. Soc.* **1999**, *121*, 8843–8854; b) G. D. Blundred, A. B. Bridges, M. J. Rosseinsky, *Angew. Chem.* **2004**, *116*, 3646–3649; *Angew. Chem. Int. Ed.* **2004**, *43*, 3562–3565; c) V. V. Poltavets, K. A. Lokshin, S. Dikmen, M. Croft, T. Egami, M. Greenblatt, *J. Am. Chem. Soc.* **2006**, *128*, 9050–9051; d) A. Bowman, M. Allix,

D. Pelloquin, M. J. Rosseinsky, *J. Am. Chem. Soc.* **2006**, *128*, 12606 – 12607.
[11] M. A. Hayward, E. J. Cussen, J. B. Claridge, M. Bieringer, M. J. Rosseinsky, C. J. Kiely, S. J. Blundell, I. M. Marshall, F. L. Pratt, *Science* **2002**, *295*, 1882 – 1884.
[12] a) T. Siegrist, S. M. Zahurak, D. W. Murphy, D. W. Roth, *Nature* **1988**, *334*, 231 – 232; b) M. Takano, T. Takeda, H. Okada, M. Miyamoto, T. Kusaka, *Physica C* **1989**, *159*, 375 – 378.
[13] a) P. K. Gallagher, J. B. MacChenney, D. N. E. Buchanan, *J. Chem. Phys.* **1966**, *45*, 2466 – 2471; b) S. E. Dann, M. T. Weller, D. B. Currie, *J. Solid State Chem.* **1992**, *97*, 179 – 185.
[14] a) P. Adler, *J. Solid State Chem.* **1997**, *130*, 129 – 139; b) L. Mogni, J. Fouletier, F. Prado, A. Caneiro, *J. Solid State Chem.* **2005**, *178*, 2715 – 2723; c) V. M. Zainullina, M. A. Korotin, V. L. Kozhevnikov, *Eur. Phys. J. B* **2006**, *49*, 425 – 431.
[15] J. F. Mitchell, J. E. Millburn, M. Medarde, S. Short, J. D. Jorgensen, M. T. Fernández-Díaz, *J. Solid State Chem.* **1998**, *141*, 599 – 603.
[16] R. LeToquin, W. Paulus, A. Cousson, C. Prestipino, C. Lamberti, *J. Am. Chem. Soc.* **2006**, *128*, 13161 – 13174.
[17] M. A. Hayward, M. J. Rosseinsky, *Nature* **2007**, *450*, 960 – 961.
[18] F. Izumi, T. Ikeda, *Mater. Sci. Forum* **2000**, *321–324*, 198 – 203.
[19] J. Rodríguez-Carvajal, *J. Phys. B* **1993**, *192*, 55 – 69.
[20] I. D. Brown, D. Altermatt, *Acta Crystallogr. Sect. B* **1985**, *41*, 244 – 247.

